



## Research on the Cross-Scale Calculation to Characterize the Fatigue-Repair Competition Mechanism of Nanoscale Modified Natural Asphalt

Xingke Zhang<sup>1,\*</sup>

<sup>1</sup> Faculty of Civil Engineering, Universiti Teknologi Malaysia, UTM, Johor, Johor Bahru, 81310, Malaysia

**SUMMARY:** *In the context of increasingly complex road service environments and enhanced requirements for high durability maintenance, the precise characterization of the fatigue-healing competition mechanism of nanomodified natural asphalt has become an important issue in material optimization. This paper integrates computer technologies such as molecular dynamics, cross-scale parameter mapping, damage driving function, competition state discrimination, and experimental-simulation collaborative calibration to construct a molecular-phase-state-microscopic-macroscopic coupled analysis framework. The results show that the dynamic modulus of group G3 reaches 2.36 GPa, the fatigue life is  $7.10 \times 10^4$  times, and the healing recovery rate is 66.9%, which demonstrates better anti-damage and recovery capabilities compared to group G0; the prediction errors of the model for fatigue life and healing recovery rate are both controlled within 4%. The research indicates that cross-scale calculations can effectively reveal the main controlling path of the fatigue-healing competition of nanomodified natural asphalt, and have theoretical and engineering significance for the design and intelligent optimization of high durability asphalt materials.*

*Povzetek:* *This paper focuses on the fatigue-healing competition mechanism of nanomodified natural asphalt, and constructs a cross-scale computational and experimental collaborative analysis framework involving molecular, phase state, microstructure and macroscopic coupling. It reveals the transmission relationship among interface interaction, phase state reorganization, crack propagation and performance evolution. Through model calibration, result verification and sensitivity analysis, the key control factors are identified, providing theoretical method support for the optimization design of high durability asphalt materials.*

**KEYWORDS:** *Cross-scale calculation; Nano-modified natural asphalt; Fatigue-healing competition mechanism; Molecular dynamics; Damage evolution; Self-healing behavior*

## 1 Introduction

In the context of continuously increasing traffic loads, increasingly complex service environments, and escalating green maintenance demands, the durability issue of asphalt materials has become a core concern in the field of road engineering. Fatigue cracking, as an important manifestation of early damage in asphalt pavements, directly affects the structural bearing capacity, service life, and maintenance costs. Meanwhile, asphalt materials possess certain self-healing potential. Processes such as internal light component migration, molecular chain rearrangement, and interface bonding recovery can promote the closure of some microcracks and the restoration of performance under suitable temperature, time, and stress

\*kke21154@163.com

<https://doi.org/10.65102/is2026092>

conditions. The fatigue damage and self-healing behavior are not isolated from each other but occur alternately and mutually restrict each other during the material's service life, ultimately jointly determining the macroscopic performance evolution of the asphalt system.

Natural asphalt, due to its stable composition, strong polarity, and good adhesion properties, has significant advantages in improving the high-temperature stability and structural strength of base asphalt. However, the incorporation of natural asphalt may also cause an increase in stiffness, changes in dispersion, and phase structure reconfiguration, thereby having a dual impact on fatigue crack resistance and healing efficiency. In recent years, nanomaterials have been widely used in asphalt modification research due to their large specific surface area, strong interface effects, and diverse control pathways. The introduction of nanoparticles can affect the asphalt colloid structure, interfacial interactions, and multi-scale energy transfer processes, resulting in more complex co-evolution characteristics at the molecular, phase, microscopic, and macroscopic levels in the modified natural asphalt system. Thus, the fatigue-healing behavior of nano-modified natural asphalt is not a linear response of a single performance indicator but a comprehensive result of multi-scale structural changes.

Most existing studies focus on fatigue performance testing, healing recovery evaluation, or analysis of certain scale mechanisms. Although they provide a foundation for understanding asphalt damage and recovery, there are two shortcomings: first, there is a lack of effective communication between different scales, making it difficult to directly explain macroscopic performance differences based on the molecular layer mechanism; second, the competition relationship between fatigue and healing under coexisting conditions, such as who dominates, when it transforms, and which factors control it, is still insufficiently depicted. Especially in nano-modified natural asphalt systems, component evolution, interface reorganization, and damage expansion are coupled, and traditional single-scale experiments or empirical analysis methods are unable to fully reveal their inherent laws.

Based on this, this paper takes nano-modified natural asphalt as the research object, focusing on the core issue of fatigue-healing competition mechanism, and constructs a cross-scale computational and experimental collaborative analysis framework to systematically reveal the intrinsic connections between the material's molecular structure, phase evolution, microscopic damage expansion, and macroscopic performance response. The research focuses include the construction of cross-scale characterization models, the depiction of fatigue-healing competition behavior, the extraction of quantitative indicators, and the sensitivity analysis of key parameters, and combines multi-scale experimental results to calibrate and validate the model. The aim is to provide theoretical basis and method support for the mechanism understanding, material optimization design, and construction of high-durability roads of nano-modified natural asphalt.

## **2 Theoretical Basis and Related Research**

### **2.1 Molecular Structure and Phase Evolution Foundation of Nano-modified Natural Asphalt**

Nano-modified natural asphalt is essentially a multi-phase composite system composed of base asphalt, natural asphalt components, and nanoparticles. Its internal structure evolution has obvious cross-scale characteristics. The saturated fraction, aromatic fraction, resin, and asphaltene in the base asphalt maintain colloid equilibrium. The introduction of natural asphalt increases the proportion of polar components in the system, enhancing intermolecular forces and exhibiting higher structural density and stronger interface adhesion. Nanoparticles, due to their large specific surface area and surface activity, can form adsorption layers with asphaltene

and resin, changing the local free volume distribution and chain segment movement ability, thereby promoting the evolution of the system from a relatively loose dispersed state to a stable aggregated state. This process not only affects the viscoelastic response of the material, but also alters the molecular migration conditions during the initiation, propagation and subsequent healing of microcracks.

From a molecular perspective, the structural stability and component compatibility of nanomodified natural asphalt are closely related. Generally, the compatibility between different components can be characterized by the solubility parameter, which is expressed as:

$$\delta = \left( \frac{E_{coh}}{V_m} \right)^{1/2} \quad (1)$$

where,  $\delta$  is the solubility parameter,  $E_{coh}$  is the cohesive energy, and  $V_m$  is the molar volume. The closer  $\delta$  is, the easier it is for the matrix asphalt, natural asphalt and nanomaterials to form a stable phase structure. Further, the interfacial interaction energy can be used to evaluate the binding strength between nanoparticles and the asphalt system:

$$E_{int} = E_{total} - E_{asphalt} - E_{nano} \quad (2)$$

In the equation,  $E_{int}$  represents the interfacial interaction energy,  $E_{total}$  is the total energy of the composite system,  $E_{asphalt}$  is the energy of the asphalt phase, and  $E_{nano}$  is the energy of the nano-phase. The larger the absolute value of  $E_{int}$ , the stronger the interfacial binding, which is more conducive to the formation of a stable multi-scale phase state network. The key components and phase-state action characteristics of nano-modified natural asphalt are shown in Table 1.

*Table 1: Key Components and Phase-State Action Characteristics of Nano-modified Natural Asphalt*

| Component                  | Structural Feature  | Main Action Scale                   | Phase State Evolution Manifestation                                | Effect on Fatigue - Healing Behavior                                   |
|----------------------------|---|-------------------------------------|--|--|
| Base asphalt               | Significant colloid system, coexistence of light components | At the molecular/ macroscopic level | Maintaining basic flow and viscoelastic balance                    | Providing fatigue energy dissipation and healing flow foundation       |
| Natural asphalt            | Strong polarity, more hard components                       | At the molecular/ phase level       | Improving the density and adhesion of the system                   | Preventing crack propagation, but may reduce the flow healing rate     |
| Nanoparticles              | High specific surface area, strong interfacial activity     | At the molecular/ microscopic level | Forming adsorption layers and strengthening interfacial connection | Enhancing structural stability, regulating fatigue and healing balance |
| Interface transition layer | There is energy exchange and chain segment reorganization   | At the phase/ microscopic level     | Promoting local structural reconstruction                          | Deciding crack closure and recovery efficiency                         |

## 2.2 Coupling mechanism and competitive criterion of fatigue damage and self-healing

Under the combined action of cyclic loading and temperature fluctuations, nano-modified natural asphalt will simultaneously undergo fatigue damage accumulation and self-healing recovery processes. Fatigue damage is mainly manifested as the gradual relaxation of weak intermolecular bonds, enhanced local stress concentration, and the initiation and expansion of microcracks; self-healing is reflected in the migration of light components, reordering of molecular chains, and reestablishment of interfacial adhesion, restoring part of the structural integrity and mechanical properties of the damaged area within a certain period of time. These two mechanisms do not exist independently but alternate and mutually restrict each other during the material's service life. When the damage propagation rate is higher than the structural recovery rate, the macroscopic performance of the material shows continuous attenuation; when the interface reorganization and molecular diffusion are strong, the stress at the crack tip can be partially released, and the system will exhibit certain recovery ability. The coupling mechanism and characterization indicators of fatigue damage and self-healing are shown in Table 2.

To quantitatively describe the evolution process of fatigue damage, the damage variable can be defined as:

$$D = 1 - \frac{S_n}{S_0} \quad (3)$$

In the formula,  $D$  represents the damage variable,  $S_0$  is the initial stiffness, and  $S_n$  is the stiffness after the  $n$ th cycle. The larger  $D$  is, the higher the cumulative degree of damage in the system.

To characterize the healing and recovery effect, the healing index can be defined as:

$$H = \frac{P_h - P_d}{P_0 - P_d} \times 100\% \quad (4)$$

In the formula,  $H$  represents the healing index,  $P_0$  is the initial performance value,  $P_d$  is the performance value after damage, and  $P_h$  is the performance value after healing. The higher the  $H$  value, the stronger the material's recovery ability.

Furthermore, a fatigue-healing competition criterion can be constructed:

$$C = \frac{H}{D} \quad (5)$$

In the formula,  $C$  represents the competition coefficient. When  $C > 1$ , cooperative effect dominates; when  $C < 1$ , fatigue damage dominates; when  $C \approx 1$ , it indicates that the system is in a dynamic competitive equilibrium state. This criterion can provide a unified basis for subsequent cross-scale quantitative analysis and model verification.

*Table 2: Coupling mechanism and characterization indicators corresponding to fatigue damage and self-healing*

| Mechanism category         | Primary manifestation   | Dominant scale                   | Typical characterization parameters                    | Effect on competitive relationship   |
|----------------------------|---|----------------------------------|--|--------------------------------------|
| Cumulative fatigue damage  | Generation and expansion of microcracks and stiffness attenuation | Fine scale/Macro scale           | Damage variables, modulus attenuation rate, cycle life | Propagates performance degradation   |
| Self-healing recovery      | Crack closure, molecular migration and interface reorganization   | Molecular/Phase state/Fine scale | Healing index, recovery rate, adhesion work            | Promotes structural repair           |
| Damage-healing competition | Synchronous evolution of the two processes                        | Inter-scale                      | Competition coefficient, recovery-decay ratio          | Determines the final evolution trend |

### 2.3 Related Work

Domestic and foreign scholars have conducted extensive research on fatigue damage, self-healing behavior and nano-modification mechanisms of asphalt materials. Chaudhary et al. (2025) focused on the influence of nano-modifying agents on the self-healing and fatigue performance of asphalt binders, indicating that the fatigue response and self-healing ability of the material would change significantly after the introduction of nano-components, providing a research basis for nano-scale regulation of asphalt service performance [1]. Chen et al. (2025) conducted multi-scale indoor experimental analysis on the self-healing behavior of steel slag asphalt mixtures under microwave heating conditions, indicating that revealing the structural recovery process from a multi-scale perspective is feasible [2]. He et al. (2021) studied the physical properties and anti-aging characteristics of nano-TiO<sub>2</sub>/Irganox 1010 composite modified asphalt, indicating that the nano-composite modification can play a positive role in structural stability and durability maintenance [3].

In terms of microscopic mechanism analysis, Yuan et al. (2024) analyzed the self-healing mechanism of TB composite modified asphalt based on molecular dynamics methods, providing a microscopic basis for explaining the connection between molecular migration, interface reorganization and recovery behavior [4]. Shu et al. (2025) studied the problem of self-healing performance degradation of asphalt mixtures under fatigue action from the perspectives of mechanism analysis and quantitative characterization, indicating that fatigue accumulation not only weakens the material's bearing capacity but also reduces its subsequent recovery potential [5]. Qinbao et al. (2025) explored the influence of graphene oxide on the rheology and self-healing performance of modified asphalt, further demonstrating the advantages of nano-materials in regulating viscoelastic characteristics and recovery behavior [6].

In addition, Zhang et al. (2023) studied the microstructure, fatigue and self-healing performance evolution of SBS modified asphalt under ultraviolet radiation conditions, indicating that environmental aging factors would significantly change the fatigue-healing relationship [7]. Yang et al. (2024) evaluated the fatigue-healing performance of fiber-modified asphalt mixtures, expanding the scope of research on damage recovery synergy in modified systems [8]. Zhang et al. (2025) analyzed the influence of aging on the structure and performance of SBS modified asphalt with dual dynamic chemical bond self-healing

reinforcement, indicating a close relationship between chemical bond design and structural response [9]. The progress and shortcomings of related research are shown in Table 3.

Table 3: Analysis of Related Research Progress and Shortcomings

| Reference | Research Object                                  | Research Perspective/Method                          | Primary Focus                              | Existing Shortcomings  |
|-----------|--|--|--|--|
| [1]       | Nanomodified asphalt binder                      | Performance tests                                    | Healing and fatigue performance            | Insufficient in revealing the multi-scale mechanism                                    |
| [2]       | Steel slag asphalt mixture                       | Multi-scale indoor tests                             | Microwave heating self-healing             | Overemphasizes external field excitation conditions, with limited material types       |
| [3]       | Nano-TiO <sub>2</sub> composite modified asphalt | Physical and anti-aging tests                        | Stability and durability                   | Does not deeply discuss the fatigue-healing coupling relationship                      |
| [4]       | TB composite modified asphalt                    | Molecular dynamics                                   | Healing micro-mechanism                    | Insufficient macroscopic response verification   |
| [5]       | Asphalt mixture                                  | Mechanism analysis and quantitative characterization | Fatigue-induced healing degradation        | Overemphasizes degradation results, with insufficient unified competitive criteria     |
| [6]       | Graphene oxide modified asphalt                  | Flowability and healing analysis                     | Nanometer regulation effect                | Insufficient discussion on phase evolution and multi-scale connection                  |
| [7]       | SBS modified asphalt                             | Structural and environmental effect analysis         | Ultraviolet aging fatigue and healing      | More emphasizes environmental factors, with less involvement of natural asphalt system |
| [8]       | Fiber modified asphalt mixture                   | Performance evaluation                               | Fatigue-healing synergy performance        | Insufficient micro-mechanism support   |
| [9]       | Self-healing reinforced SBS modified asphalt     | Structure and performance analysis                   | Aging influence and dynamic chemical bonds | Still insufficient characterization of cross-scale competitive mechanism               |

Overall, existing research has explored the issues of asphalt fatigue and healing from perspectives such as nano-modification, microwave heating, molecular dynamics, flow analysis, and aging environment. However, it is still mainly focused on single material systems, single-scale analysis, or local performance evaluation. For the composite system of nano-modified natural asphalt, especially the competitive mechanism and cross-scale characterization under the condition of concurrent fatigue damage and self-healing, there is still a lack of systematic and unified research framework. Therefore, it is necessary to further

construct an analysis method that covers multi-level coupling from molecular to phase state to microstructure to macroscopic levels to achieve quantitative depiction of the fatigue-healing competitive mechanism.

### 3 Cross-scale computational-driven study on the fatigue-healing competition mechanism of nano-modified natural asphalt

#### 3.1 Construction of a cross-scale characterization model integrating molecular, phase state, microscale and macroscale

To reveal the transmission law of structural evolution to performance response of nano-modified natural asphalt under fatigue loading, this paper constructs a four-level coupling cross-scale characterization model integrating molecular, phase state, microscale and macroscale. The effects of micro-component action, phase state reorganization, crack damage expansion and macroscopic mechanical degradation are unified into the same analysis framework. The model starts from the interface interaction between nanoparticles, active components of natural asphalt and the colloid structure of the matrix asphalt, extracts parameters such as interface interaction energy, diffusion ability and local binding stability at the molecular scale, and maps them to the phase state scale to characterize the structural evolution characteristics of different components during aggregation, dispersion and reorganization [10]. Further, by transferring local heterogeneous information from the phase state scale to the microscale, a characterization channel for the coordinated evolution of crack initiation, expansion and interface recovery is established, and finally, the unified prediction of modulus attenuation, fatigue life and healing recovery rate indicators is achieved at the macroscopic scale. The framework of the molecular-phase-state-microscale-macroscopic coupling cross-scale characterization model is shown in Figure 1.

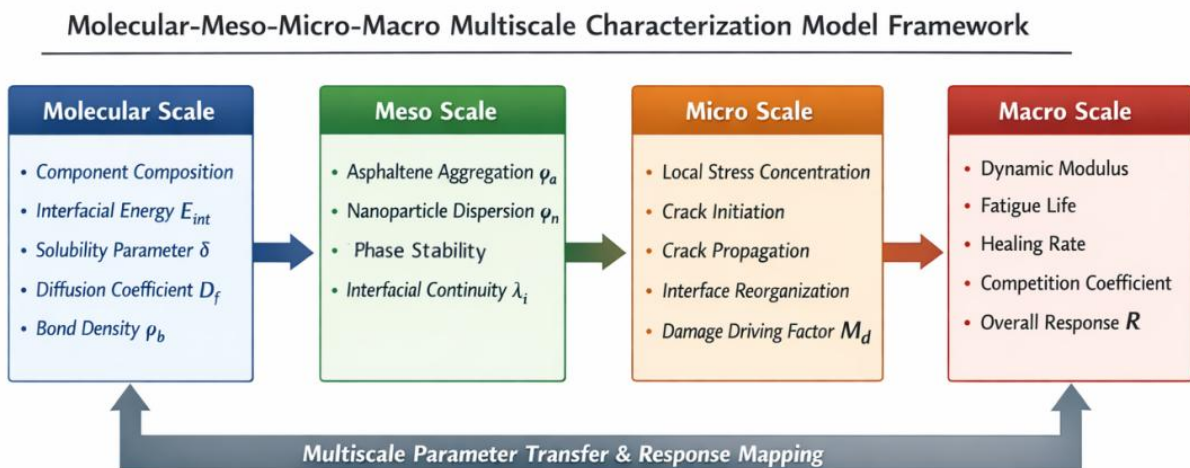


Figure 1: Cross-scale characterization model framework of molecular-phase-state-microscopic-macroscopic coupling

At the molecular scale, the state vector of the nano-modified natural asphalt system is defined as:

$$X_m = [E_{\text{int}}, \delta, D_f, \rho_b] \quad (6)$$

where,  $X_m$  is the molecular-scale state vector,  $E_{\text{int}}$  is the interfacial interaction energy,  $\delta$  is the solubility parameter,  $D_f$  is the molecular diffusion coefficient, and  $\rho_b$  is the local binding density. This vector is used to describe the compatibility and binding stability of nanoparticles and natural asphalt components at the molecular level, providing the underlying input for subsequent phase-state reconstruction.

At the phase-state scale, the molecular-scale parameters are mapped to phase-state characterization quantities, and a phase-state state vector is constructed:

$$X_p = [\phi_a, \phi_n, \eta_s, \lambda_i] \quad (7)$$

where,  $X_p$  is the phase-state scale state vector,  $\phi_a$  is the asphalt aggregation degree,  $\phi_n$  is the dispersion coefficient of nanoparticles,  $\eta_s$  is the phase structure stability index, and  $\lambda_i$  is the continuity parameter of the interface transition layer. The relationship between molecular parameters and phase-state parameters can be established through a mapping function:

$$X_p = T_{mp} X_m \quad (8)$$

In the equation,  $T_{mp}$  is the coupling transfer matrix from the molecular scale to the phase-scale, which is used to represent the mapping relationship between interfacial energy, diffusion characteristics, and phase structure stability.

At the microscale, considering factors such as local stress concentration, discontinuity of the phase interface, and microcrack propagation, the microscale damage state quantity is defined as:

$$M_d = \alpha\phi_a + \beta(1 - \phi_n) + \gamma(1 - \lambda_i) \quad (9)$$

In this equation,  $M_d$  is the microscale damage driving factor, and  $\alpha$ ,  $\beta$ , and  $\gamma$  are weight coefficients. This equation indicates that the enhancement of asphalt aggregation, the insufficiency of nano-dispersion, and the decline in interface continuity will all increase the local damage sensitivity and promote the evolution of cracks from initiation to the expansion stage. At the same time, if the molecular diffusion ability and interface binding stability remain at a high level, the local damaged area still has certain potential for reorganization and recovery, thereby forming a competitive situation where fatigue damage and self-healing coexist.

At the macroscale, this paper further maps the cross-scale features into the material mechanical response and establishes a comprehensive characterization function:

$$R = \omega_1 M_d + \omega_2 \eta_s + \omega_3 E_{\text{int}} + \omega_4 D_f \quad (10)$$

In this equation,  $R$  is the macroscopic response characterization value, and  $\omega_1$  to  $\omega_4$  are the weight coefficients of each scale feature. Depending on different research goals,  $R$  can correspond to output indicators such as dynamic modulus, fatigue life, healing recovery rate, or competitive coefficient. The core of this model lies in integrating the microscopic structure information, phase evolution characteristics, and microscale damage state into the macroscopic performance expression, enabling the fatigue-healing behavior of nanomodified natural asphalt no longer to rely solely on a single experimental result for judgment, but to be systematically characterized through the linkage of cross-scale parameters.

To improve the interpretability and computability of the model, this paper introduces a four-stage path of "parameter extraction - scale mapping - damage characterization - macroscopic

response" during model construction. This path retains the analytical advantage of molecular simulation for interface mechanisms, takes into account the physical meanings of phase reorganization and microscale damage expansion, and can be calibrated with subsequent experimental data [11]. Through this cross-scale characterization model, a unified method basis can be provided for the quantitative analysis of the fatigue-healing competitive mechanism of nanomodified natural asphalt, and a model support can be laid for the subsequent characterization of competitive behavior and the construction of key indicators.

### 3.2 Characterization Method for Fatigue-Healing Competitive Behavior Based on Damage Evolution and Interface Reorganization

Under the combined action of cyclic loading, intermittent recovery time, and temperature, in nanomodified natural asphalt, internal damage does not only occur in a unidirectional manner but presents a dynamic competitive process of "crack propagation - interface reorganization - local recovery". During the fatigue stage, local stress concentration prompts the priority damage of weak interface regions, and microcracks gradually expand in the microheterogeneous structure; in the healing stage, molecular chain segment migration, redistribution of light components, and interface adhesion reconstruction around the nanoparticles will partially weaken the driving force at the crack tip, causing a certain degree of closure and recovery in the damaged area [12]. Based on this feature, this paper regards the fatigue-healing competitive behavior as a coupled evolution problem of the "damage growth term" and "interface recovery term", and establishes a behavior characterization method based on the cross-scale parameter transfer. The key processes and model parameters in the characterization of fatigue-healing competitive behavior are shown in Table 4.

*Table 4: Key Processes and Model Parameter Settings in Fatigue-Healing Competitive Behavior Characterization*

| Process category                  | Primary physical meaning  | Primary parameter name          | Suggested range of values     | Role in the competitive behavior                                  |
|-----------------------------------|---|---------------------------------|-------------------------------|---|
| Local damage accumulation         | Expansion of micro-defects and structural weakening under cyclic loading    | Damage evolution coefficient    | 0.015~0.035                   | Controls the growth rate of fatigue damage                        |
| Local damage accumulation         | Expansion of micro-defects and structural weakening under cyclic loading    | Local equivalent stress ratio   | 0.72~0.91                     | Reflects the degree of stress concentration                       |
| Local damage accumulation         | Expansion of micro-defects and structural weakening under cyclic loading    | Damage driving level            | 0.40~0.68                     | Characterizes the sensitivity of crack initiation and propagation |
| Phase-state stability constraint  | Inhibition of damage propagation by phase-structure continuity              | Phase-structure stability level | 0.63~0.86                     | Delays the evolution of local damage                              |
| Phase-state stability constraint  | Inhibition of damage propagation by phase-structure continuity              | Interface continuity level      | 0.58~0.82                     | Enhances overall structural coordination                          |
| Interface reorganization recovery | Reconstruction of interfacial adhesion and crack closure                    | Interface reorganization rate   | 0.020~0.048 min <sup>-1</sup> | Controls the recovery rate of healing                             |
| Interface reorganization recovery | Reconstruction of interfacial adhesion and crack closure                    | Recovery time                   | 10~60 min                     | Determines the adequacy of interface reconstruction               |
| Interface reorganization recovery | Reconstruction of interfacial adhesion and crack closure                    | Interfacial interaction level   | 1.12~1.38                     | Represents the enhancement capability of interfacial adhesion     |
| Molecular migration support       | Promotion of recovery by diffusion of light components and molecular chains | Molecular diffusion level       | 0.78~1.21                     | Affects mass transfer efficiency during the healing stage         |
| Molecular migration support       | Promotion of recovery by diffusion of light components and molecular chains | Migration activation level      | 0.46~0.73                     | Reflects the mobility of molecular chain segments                 |
| Competitive state identification  | Comprehensive judgment of fatigue- or healing-dominated trend               | Net driving level               | -0.25~0.37                    | Determines whether crack propagation or recovery is dominant      |
| Competitive state                 | Comprehensive judgment of fatigue- or                                       | Competition state               | -0.30~0.45                    | Outputs fatigue-dominated,  |

|                |                         |       |  |                                       |
|----------------|-------------------------|-------|--|---------------------------------------|
| identification | healing-dominated trend | index |  | balanced, or healing-dominated states |
|----------------|-------------------------|-------|--|---------------------------------------|

To describe the cumulative damage state under cyclic loading, the normalized fatigue damage function is defined as:

$$\Omega(N) = 1 - \exp \left[ -k_d N \left( \frac{\sigma_{loc}}{\sigma_c} \right)^m \frac{M_d}{\eta_s + \lambda_i} \right] \quad (11)$$

where,  $\Omega(N)$  is the damage state function under the  $N$ th cycle,  $k_d$  is the damage evolution coefficient,  $\sigma_{loc}$  is the local equivalent stress,  $\sigma_c$  is the critical stress,  $m$  is the stress sensitivity index,  $M_d$  is the microscopic damage driving factor,  $\eta_s$  is the phase structure stability index, and  $\lambda_i$  is the interface continuity parameter. This equation indicates that when the local stress level increases and the microstructure heterogeneity enhances, the damage growth rate will significantly accelerate; while higher phase state stability and interface continuity will help delay the accumulation of damage.

Considering the combined influence of interface adhesion reconstruction and molecular migration during the healing stage, the interface reformation coefficient is further defined as:

$$\Psi(t_r) = \lambda_i (1 - e^{-k_h t_r}) \left( \frac{E_{int}}{E_{ref}} \right)^p \left( \frac{D_f}{D_{ref}} \right)^q \quad (12)$$

where,  $\Psi(t_r)$  is the interface reformation coefficient during the recovery time  $t_r$ ,  $k_h$  is the interface reformation rate constant,  $E_{int}$  is the interface interaction energy,  $E_{ref}$  is the reference interface energy,  $D_f$  is the molecular diffusion coefficient,  $D_{ref}$  is the reference diffusion coefficient,  $p$  and  $q$  are weight indices. This equation explains that an extended recovery time, enhanced interface interaction, and improved molecular diffusion ability will all increase the interface reformation level, thereby enhancing the healing potential of the material.

To further depict the competitive relationship between crack propagation and interface reformation, the net driving function is defined as:

$$F_{net} = G_0 \Omega(N) - \mu \Psi(t_r) \quad (13)$$

where,  $F_{net}$  is the fatigue-healing net driving function,  $G_0$  is the initial crack driving benchmark term, and  $\mu$  is the reduction coefficient of the interface reformation on the crack driving force. When  $F_{net} > 0$ , it indicates that the fatigue propagation effect is dominant, and the crack tends to develop further; when  $F_{net} < 0$ , it means that the interface reformation has a strong inhibitory effect on crack propagation, and the system is more likely to enter the dominance of recovery.

Based on this, the competitive state discrimination function is constructed:

$$\Theta = \omega_1 \Omega(N) - \omega_2 \Psi(t_r) + \omega_3 \frac{F_{net}}{G_0} \quad (14)$$

In the formula,  $\Theta$  represents the competition state factor, while  $\omega_1$ ,  $\omega_2$ , and  $\omega_3$  are weight coefficients. Considering the need to form a unified output indicator in the subsequent multi-scale parameter fusion calculation, this paper takes  $\Theta$  as the intermediate discriminant quantity in the competition process. Its positive and negative directions are consistent with the competition state coefficient  $\Gamma$  in Section 3.3. When  $\Theta < 0$ , it indicates that the fatigue expansion effect is dominant, and the system as a whole shows fatigue dominance; when  $\Theta > 0$ , it indicates that the recovery effect corresponding to interface reorganization and molecular migration is stronger, and the system shows healing dominance; when  $\Theta \approx 0$ , it can be

considered that the material is in a competitive state where fatigue and healing are balanced [13]. Compared with merely relying on a single recovery rate or stiffness attenuation rate for judgment, this method can simultaneously incorporate cross-scale information such as local stress, phase stability, interfacial energy, and diffusion behavior, and provide a process discriminant basis for the unified calculation of the competition state coefficient  $\Gamma$  in Section 3.3.

### 3.3 Multi-scale Parameter Fusion for Fatigue-Hybridization Competition State Discrimination and Computational Flow Design

After completing the construction of the cross-scale representation model and the characterization of fatigue-hybridization competition behavior, it is necessary to establish a set of state discrimination methods that can connect the molecular scale, phase state scale, microscale and macroscopic response, enabling parameters from different sources to be fused, calculated and output within a unified framework. For nanomodified natural asphalt, fatigue propagation is not solely determined by the load level; interface reorganization, molecular migration, phase structure stability and local crack evolution all jointly affect the competition state [14]. Therefore, in this section, starting from multi-scale parameter fusion, a fatigue-hybridization competition state discrimination and computational flow is constructed, converting the molecular interaction information, phase structure information and microdamage information in the aforementioned model into computable state functions. The fatigue-hybridization competition state discrimination and computational flow based on multi-scale parameter fusion is shown in Figure 2.

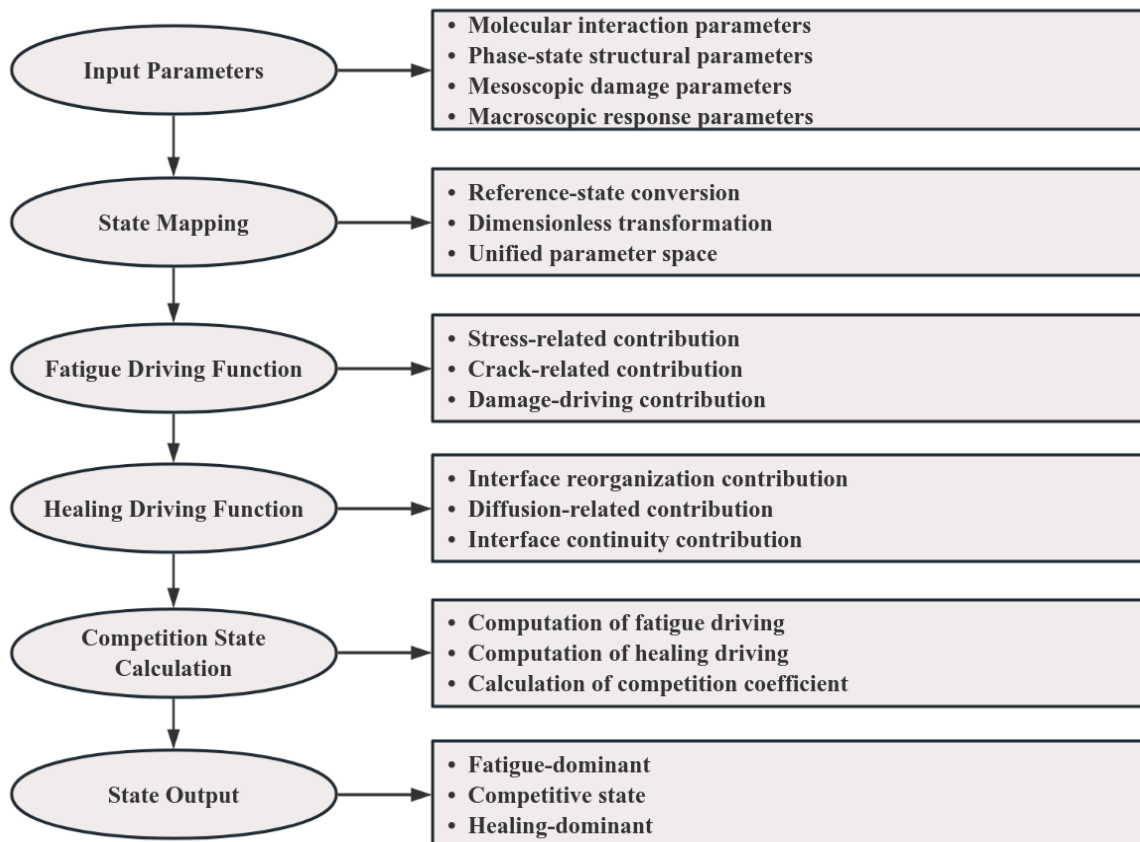


Figure 2: Flowchart of fatigue-healing competition state discrimination and calculation based on multi-scale parameter fusion

Taking into account the differences in dimension, range, and physical meaning of different scale parameters, the input parameters are first uniformly mapped, and the standard state quantity before fusion is defined as:

$$y_i = \frac{x_i}{x_i + x_i^{\text{ref}}} \quad (15)$$

In this equation,  $y_i$  represents the standard state quantity of the  $i$ -th parameter,  $x_i$  is the original input parameter, and  $x_i^{\text{ref}}$  is the reference state value. This equation can avoid the direct superposition deviation caused by the dimensional differences of different parameters, allowing information such as the interface action level, phase structure stability degree, local stress concentration level and diffusion ability to enter the same calculation space.

Based on this, the fatigue driving function is defined as:

$$P_f = c_1 y_s + c_2 y_c + c_3 y_m \quad (16)$$

In the formula,  $P_f$  is the fatigue driving function,  $y_s$  is the stress level mapping value,  $y_c$  is the crack evolution-related state quantity, and  $y_m$  is the microscopic damage driving state quantity.  $c_1$ ,  $c_2$ , and  $c_3$  are corresponding weights. This function is used to characterize the overall trend of the system's evolution towards the damage expansion direction under cyclic loading, and the larger the value, the more obvious the fatigue expansion tendency within the material.

Correspondingly, the healing driving function is defined as:

$$P_h = d_1 y_r + d_2 y_d + d_3 y_l \quad (17)$$

In the formula,  $P_h$  is the healing driving function,  $y_r$  is the interface reorganization state quantity,  $y_d$  is the molecular migration ability mapping value,  $y_l$  is the interface continuity state quantity, and  $d_1$ ,  $d_2$ ,  $d_3$  are corresponding weights. This function mainly reflects the potential of the material to achieve local repair through interface adhesion reconstruction and light component diffusion during the recovery stage.

To further unify the description of the competition between fatigue and healing, a competitive state coefficient is constructed:

$$\Gamma = \frac{P_h - P_f}{P_h + P_f + \varepsilon} \quad (18)$$

In the formula,  $\Gamma$  is the competitive state coefficient, and  $\varepsilon$  is a correction term to prevent the denominator from being too small and causing fluctuations. The value range of this coefficient is close to  $[-1, 1]$ . When  $\Gamma$  approaches a negative value, it indicates that fatigue propagation dominates; when  $\Gamma$  approaches a positive value, it indicates that the healing recovery effect is stronger; when  $\Gamma$  approaches zero, it indicates that the system is in a competitive state where damage and recovery are balanced.

To enable the calculation results to form clear state outputs, a hierarchical discrimination function is further set:

$$R_s = \begin{cases} \text{Fatigue – dominant,} & \Gamma < -0.15 \\ \text{Competitive state,} & -0.15 \leq \Gamma \leq 0.15 \\ \text{Healing – dominant,} & \Gamma > 0.15 \end{cases} \quad (19)$$

In this formula,  $R_s$  is the competitive state category. This discrimination method converts the continuous state coefficient into a discrete result, enabling the identification of competitive states under different material ratios, different recovery times, and different load levels in a unified standard.

In the calculation process, this paper adopts the method path of "parameter input - state mapping - double driving function construction - competitive state coefficient calculation - state classification output". The key of this path is not to regard fatigue and healing as two independent processes that are mutually separated, but to express both in a unified framework [15]. This not only retains the explanatory ability of molecular-scale interface effects and diffusion behaviors on healing and recovery, but also takes into account the stability of phase states and the evolution of micro-damage on fatigue propagation. Compared with traditional methods that only rely on a single recovery rate, stiffness decay rate, or fatigue life for judgment, the state discrimination and calculation process proposed in this section can better reflect the cross-scale coupling characteristics of the fatigue-healing competition mechanism of nanomodified natural asphalt, and is more in line with the writing positioning of the chapter as a research method chapter.

## 4 Experimental and Result Analysis

### 4.1 Material Preparation and Nanomodification Scheme and Multi-scale Characterization Test Design

To ensure the comparability between the cross-scale calculation results and the real response of the material, this paper selects 70# base asphalt as the basic material, builds a composite modification system with natural asphalt and nanomodifying agents, and conducts test design along the technical route of "material preparation - specimen molding - fatigue loading - healing and recovery - multi-scale characterization". During the preparation process, the base asphalt is heated to 160 °C and kept in a flowing state, then natural asphalt is added in the set proportion, and it is pre-mixed at high-speed shear for 30 minutes to fully disperse the hard component; then, the nanomaterial is added and further sheared for 45 minutes to promote the uniform distribution of nanomaterials in the continuous phase of the asphalt [16]. Considering that the aggregation of nanomaterials will affect the interface effect and subsequent fatigue-healing behavior, the shear temperature, rotational speed, and holding time during the preparation stage are synchronized controlled to ensure the consistency of sample preparation conditions. The material preparation and nanomodification scheme and multi-scale characterization test design are shown in Table 5.

*Table 5: Material Preparation and Nanomodification Scheme and Multi-scale Characterization Test Design*

| Group | Base asphalt / % | Natural asphalt / % | Nanomaterial / % | Preparation temperature / °C | Shear speed / (r·min <sup>-1</sup> ) | Shear time / min | Main test contents   | Corresponding scale      |
|-------|------------------|---------------------|------------------|------------------------------|--------------------------------------|------------------|--|--------------------------|
| G0    | 100.0            | 0.0                 | 0.0              | 160                          | 3000                                 | 60               | Baseline rheological, fatigue, and healing tests                     | Macroscale               |
| G1    | 94.0             | 6.0                 | 0.0              | 165                          | 3500                                 | 75               | Evaluation of natural asphalt modification effect                    | Phase state / Macroscale |
| G2    | 93.5             | 6.0                 | 0.5              | 165                          | 4000                                 | 75               | Rheological, fatigue-recovery, and microscopic observation tests     | Mesoscale / Macroscale   |
| G3    | 93.0             | 6.0                 | 1.0              | 165                          | 4000                                 | 75               | Crack evolution, interface distribution, and recovery capacity tests | Mesoscale / Macroscale   |
| G4    | 92.5             | 6.0                 | 1.5              | 165                          | 4500                                 | 90               | Multiscale collaborative characterization and model calibration      | Molecular-Macroscale     |

In the test grouping, a non-modified control group, a natural asphalt modified group, and different nano-dosage composite modified groups were set up to compare the changes in material structural stability, fatigue damage resistance, and healing recovery potential under the synergistic effect of natural asphalt and nano-materials. After the specimen was formed, dynamic shear rheology, linear amplitude scanning, and fatigue-recovery cyclic tests were conducted at the macroscopic level to obtain indicators such as modulus, damage evolution, and healing recovery rate; at the fine-scale level, fluorescence microscopy and scanning electron microscopy were used to observe crack initiation and interface distribution characteristics; at the phase/state level, thermal analysis and component separation results were combined to identify the structural evolution trend; at the molecular level, parameters related to interface interaction, diffusion migration, and binding stability were extracted to provide input for subsequent cross-scale mapping and model calibration. Through this design, the material responses at different scales can be realized to correspond and connect within the same test framework.

## **4.2 Cross-scale calculation settings and test-simulation collaborative calibration process**

To ensure that the cross-scale calculation model can truly reflect the structural evolution characteristics of nano-modified natural asphalt during fatigue and healing processes, this paper sets corresponding calculation parameters at the molecular, phase/state, fine-scale, and macroscopic levels, and conducts test-simulation collaborative calibration using the method of "test input - parameter mapping - initial value calculation - error feedback - iterative correction". The molecular layer mainly inputs interface interaction level, diffusion ability, and binding stability parameters to characterize the interaction between nano-particles and natural asphalt components; the phase/state layer focuses on setting aggregation degree, dispersion level, and

structural continuity parameters to describe the characteristics of phase structure reorganization in the system; the fine-scale layer introduces local stress concentration, crack extension sensitivity, and damage driving level; the macroscopic layer takes dynamic modulus, fatigue life, and healing recovery rate as the final response output [17]. The key parameter settings and calibration targets of cross-scale calculation are shown in Table 6.

*Table 6: Key parameter settings and calibration targets of cross-scale calculation*

| Scale level       | Parameter name                         | Initial value | Unit | Parameter source                     | Calibration objective  |
|-------------------|--|---------------|------|--------------------------------------|--|
| Molecular scale   | Interfacial interaction level          | 1.24          | —    | Molecular interaction analysis       | Improve the characterization accuracy of interfacial bonding |
| Molecular scale   | Diffusion capability                   | 0.93          | —    | Molecular migration analysis         | Reflect migration characteristics during the healing stage   |
| Phase-state scale | Structural stability level             | 0.78          | —    | Phase-state evolution identification | Characterize the balance between aggregation and dispersion  |
| Phase-state scale | Interface continuity level             | 0.74          | —    | Structural reorganization analysis   | Improve the accuracy of phase-state mapping                  |
| Mesoscale         | Damage growth coefficient              | 0.028         | —    | Crack propagation characterization   | Match the evolution trend of fatigue damage                  |
| Mesoscale         | Local stress amplification coefficient | 1.16          | —    | Mesomechanical analysis              | Correct the sensitivity of local damage                      |
| Macroscale        | Reference dynamic modulus              | 2.00          | GPa  | Rheological test                     | Calibrate stiffness prediction results                       |
| Macroscale        | Reference healing recovery value       | 61.0          | %    | Fatigue–recovery test                | Calibrate healing response results                           |

Macroscale Healing recovery reference value 61.0 % Fatigue-recovery test Calibrate healing response results During the collaborative calibration process, initially, the initial values of parameters at each level are determined based on the material preparation plan and the results of multi-scale experiments. Then, the molecular and phase state information is mapped into the microstructural damage evolution model to obtain the initial predicted results for different sample groups. Subsequently, the simulation outputs are compared with the results obtained from dynamic shear rheology tests and fatigue-recovery cycle tests. The relative error and fitting consistency are used as correction criteria, and the interface reorganization rate, structural stability level, and damage growth parameters are iteratively adjusted until the main response indicators reach a high degree of matching [18]. This not only retains the explanatory ability of cross-scale calculations for the microscopic action mechanism but also enhances the model's adaptability to macroscopic mechanical responses. The collaborative calibration comparison curve of the experimental values and simulation values is shown in Figure 3.

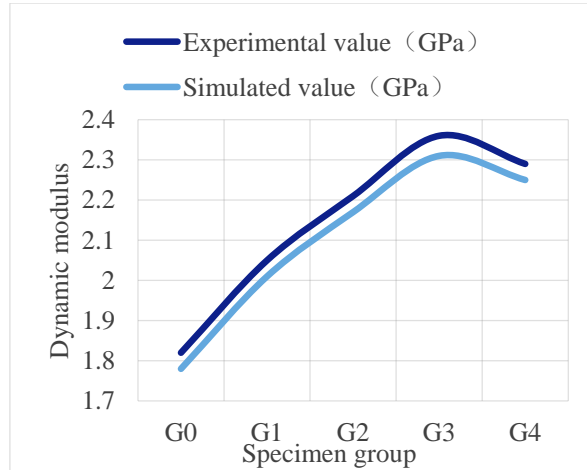


Figure 3: Coordinated calibration comparison curve of test values and simulation values

As shown in Figure 3, the dynamic modulus prediction curves of each group of samples are consistent with the overall change trend of the test curves, indicating that the constructed model can well describe the change law of the stiffness response of the material after the synergistic modification of natural asphalt and nanomaterials. Among them, the test values of G3 group are the closest to the simulation values, suggesting that under the current parameter settings, the model adequately characterizes the interface enhancement and structural stability effects under a 1.0% nano-concentration condition; G4 group shows a slight deviation, indicating that when the nano-concentration is further increased, local agglomeration and phase heterogeneity will have a certain impact on the model accuracy. Overall, the coordinated calibration process established in this section provides a reliable parameter basis for the subsequent fatigue-healing performance evolution analysis and competitive mechanism verification.

### 4.3 Comparison of Fatigue and Healing Performance Evolution Results and Model Verification

After completing the cross-scale parameter calibration, a further comparative analysis was conducted on the fatigue damage accumulation process, healing recovery ability, and model prediction accuracy of different sample groups. The fatigue damage evolution curve is shown in Figure 4, and the comparison chart of healing recovery rates is shown in Figure 5.

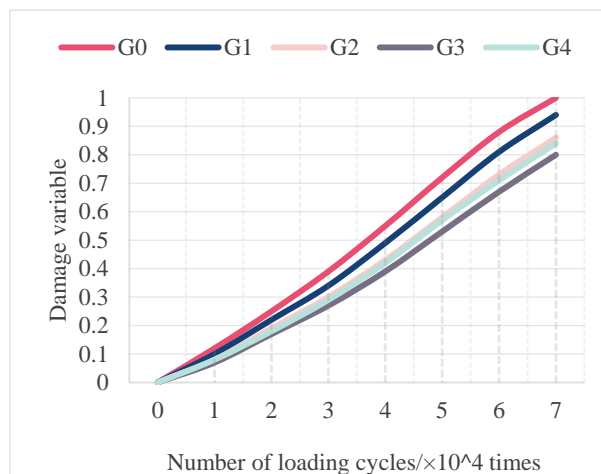


Figure 4: Fatigue Damage Evolution Curve

As shown in Figure 4, the damage variables of each group of specimens continuously increased with the continuous loading cycles, but the growth rates were significantly different. The unmodified group G0 increased the fastest, reaching a damage variable of 0.72 at  $5 \times 10^4$  cycles; while the G3 group was only 0.53 at the same time, indicating that the appropriate addition of nanomaterials in combination with natural asphalt can effectively delay the initiation and propagation of cracks. The G1 and G2 groups showed a more gradual damage growth trend compared to G0, while the G4 group was slightly better than the control group but slightly weaker than the G3 group, suggesting that when the nanomaterial content is too high, local agglomerations will weaken the interface reinforcement effect.

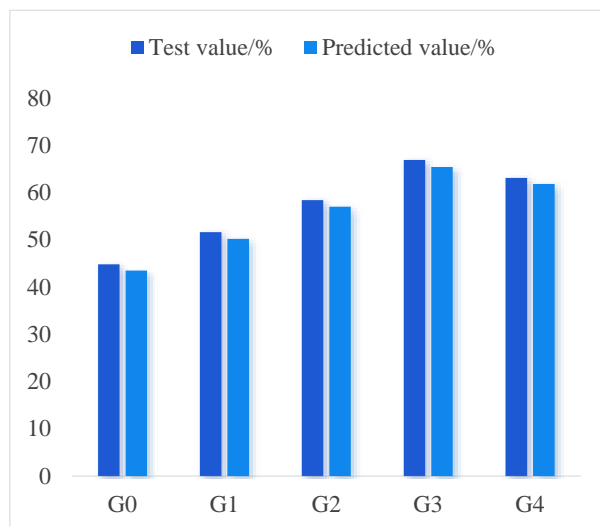


Figure 5: Comparison Bar Chart of Healing Recovery Rate

The main results are shown in Table 7.

Table 7: Comparison of Fatigue and Healing Performance and Model Verification Results

| Group | Experimental fatigue life / $\times 10^4$ cycles | Predicted fatigue life / $\times 10^4$ cycles | Relative error / % | Experimental healing recovery rate / % | Predicted healing recovery rate / % | Relative error / % |
|-------|--|---|--------------------|--|-------------------------------------|--------------------|
| G0    | 4.60   | 4.43  | 3.70               | 44.8                                   | 43.5                                | 2.90               |
| G1    | 5.30   | 5.10  | 3.77               | 51.6                                   | 50.2                                | 2.71               |
| G2    | 6.20   | 6.01  | 3.06               | 58.4                                   | 57.0                                | 2.40               |
| G3    | 7.10   | 6.90  | 2.82               | 66.9                                   | 65.4                                | 2.24               |
| G4    | 6.80   | 6.57  | 3.38               | 63.1                                   | 61.8                                | 2.06               |

From Figure 5 and Table 7, it can be seen that both the healing recovery rate and fatigue life show a pattern of increasing first and then decreasing. Among them, Group G3 has the best overall performance. Its fatigue life test value reaches  $7.10 \times 10^4$  times, which is 54.35% higher than that of Group G0; the healing recovery rate reaches 66.9%, which is 22.1 percentage points higher than that of Group G0. The model prediction results are consistent with the test results, and the relative error of fatigue life for each group is controlled within 4%, and the error of healing recovery rate is no more than 3.5%, indicating that the constructed model can accurately reflect the fatigue-healing evolution process of nano-modified natural asphalt. Overall, the synergistic effect of natural asphalt and nano-materials can enhance the

structural stability while improving the interface reorganization ability. Among them, the comprehensive balance effect under the condition of 1.0% nano-concentration is the best, providing a reliable basis for the analysis of competitive mechanism influencing factors in the future.

#### 4.4 Quantitative Results of Competitive Mechanism and Analysis of Key Influencing Factors

After completing the verification of fatigue damage evolution and healing recovery performance, further based on the aforementioned competitive state discrimination method, the competitive results of different sample groups under typical recovery conditions were analyzed. To facilitate the unified identification of the competitive states of different material systems, the discrimination interval of the competitive state coefficient  $\Gamma$  in this paper is divided into:  $\Gamma < -0.05$  as the fatigue dominant zone,  $-0.05 \leq \Gamma \leq 0.05$  as the competitive balance zone, and  $\Gamma > 0.05$  as the healing dominant zone. The calculation results show that the competitive state of each group of samples varies significantly with the modification scheme, where the competitive state coefficient of the unmodified group G0 is -0.18, which is in the fatigue dominant zone; the natural asphalt modified group G1 is raised to -0.05, which has entered the competitive balance boundary; the composite modified groups G2, G3, and G4 reach 0.08, 0.21, and 0.14 respectively, indicating that after the synergistic effect of nano-materials and natural asphalt, the system gradually shifts from the single damage expansion dominance to the fatigue-healing concurrent competition, and shows more obvious recovery advantages under the condition of 1.0% nano-concentration. The variation curves of competitive state coefficients under different recovery temperatures are shown in Figure 6, and the key influencing factor analysis results are shown in Table 8.

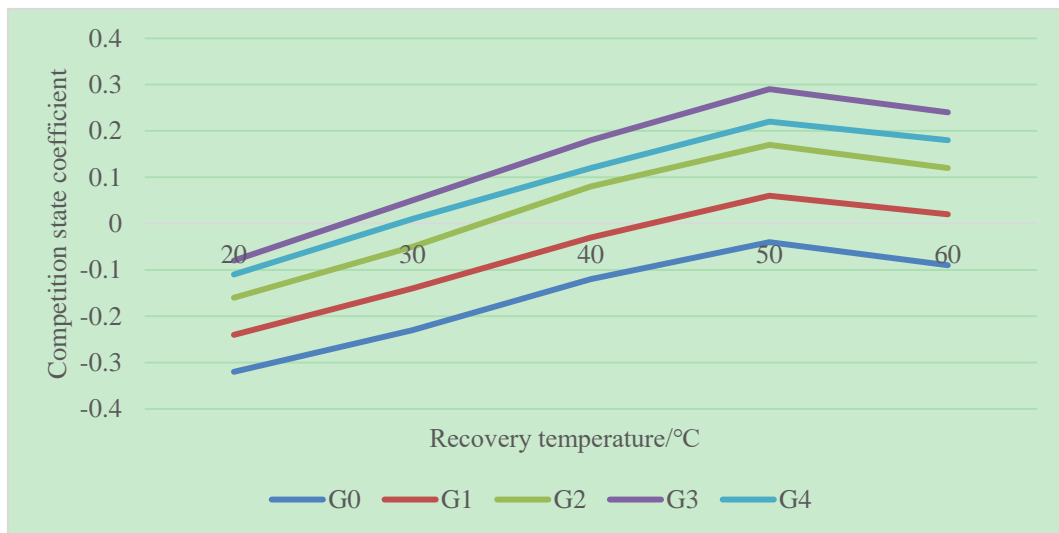


Figure 6: Line graph showing the changes in competitive state coefficients at different recovery temperatures

As shown in Figure 6, as the recovery temperature increased from 20 °C to 50 °C, the competitive state coefficients of each group of samples showed an overall upward trend, indicating that a moderate increase in temperature can enhance the molecular migration and interface reorganization ability, thereby increasing the proportion of healing effect in the

competitive relationship. Among them, the G3 group increased from -0.08 to 0.29, with the largest increase, indicating that it achieved a better balance between temperature sensitivity and structural recovery ability. The G2 group and G4 group also showed similar trends, but the increase in the high-temperature zone was slightly lower than that of the G3 group. This indicates that when the nano-dosage is insufficient, the interface enhancement is not obvious, while when the dosage is too high, local agglomeration and structural inhomogeneity will weaken the recovery efficiency. It is worth noting that when the temperature was further increased to 60 °C, the competitive state coefficients of some sample groups slightly decreased, such as G3 group from 0.29 to 0.24, and G4 group from 0.22 to 0.18. This indicates that although a higher temperature is conducive to flow and diffusion, it may also weaken the stability of the phase structure, causing the fatigue-healing competitive relationship to shift from "recovery enhancement" to "structural softening" and "local instability" coexisting.

*Table 8: Analysis results of key influencing factors*

| Influencing factor     | Parameter range | Variation range of competition state coefficient | Contribution / % | Main effect characteristic  |
|------------------------|-----------------|--|------------------|---|
| Recovery temperature   | 20–60 °C        | 0.24–0.37  | 29.4             | Significantly affects molecular migration and interface reorganization efficiency |
| Recovery time          | 10–60 min       | 0.18–0.31  | 25.7             | Determines the adequacy of the healing process                                    |
| Nanomaterial dosage    | 0–1.5%          | 0.16–0.29  | 21.8             | Regulates interfacial enhancement capability and structural stability             |
| Local stress level     | 0.70–0.95       | 0.09–0.18  | 14.3             | Influences the rate of damage propagation and the direction of competition        |
| Natural asphalt dosage | 0–8%            | 0.05–0.12  | 8.8              | Regulates system stiffness and interfacial adhesion level                         |

Based on the parameter setting range of recovery time 10-60 min in Table 4 of Section 3.2 and the calculated results of competitive state coefficients after the collaborative calibration of experiments and simulations, this paper further adopted the single-factor sensitivity analysis method to quantitatively compare the influence degree of recovery temperature, recovery time, nano dosage, local stress level and natural asphalt dosage, and obtained the contribution rate results shown in Table 8. From Table 8, it can be seen that among the key factors analyzed, recovery temperature has the greatest impact on the competitive result, with a contribution rate of 29.4%, indicating that the temperature condition directly determines the efficiency of interface reorganization and the activity of molecular migration; the contribution rate of recovery time is 25.7%, indicating that an adequate recovery stage is an important prerequisite for the effective exertion of the healing effect; the contribution rate of nano dosage is 21.8%, indicating that nanomaterials have a significant effect in constructing a stable interface and delaying fatigue expansion. In contrast, the contribution rates of local stress level and natural asphalt dosage are 14.3% and 8.8% respectively, although lower than the first three items, they still affect the final competitive state by regulating the local damage sensitivity and the stiffness level of the system. Overall, the competitive mechanism is not determined by a single factor, but is the result of the joint action of recovery conditions, material composition and local damage environment. Among them, recovery temperature, recovery time and nano dosage

constitute the main control factor combination, determining whether the material system tends towards fatigue dominance, competitive balance or healing dominance. This result further indicates that the composite modification design should not only focus on the anti-fatigue or healing single indicator, but should optimize the material ratio and recovery conditions from the perspective of multi-factor coupling to achieve a dynamic balance between fatigue inhibition and structure recovery.

## 5 Discussion

The research results of this paper indicate that the fatigue-healing competition behavior of nano-modified natural asphalt is not merely a direct manifestation of a single mechanical response, but rather a result of the coupling of molecular interactions, phase-state evolution, microscopic damage propagation, and macroscopic performance degradation. As can be seen from the results in Chapter 4, the introduction of natural asphalt enhances the overall stiffness and interface adhesion of the system, enabling the material to possess stronger damage resistance in the early fatigue stage. Nano materials further strengthen the interface bonding and structural continuity, delay crack propagation, and improve the interface reorganization efficiency during the recovery stage. This indicates that the composite modification effect is not simply additive, but rather through multi-scale structural reconstruction, it alters the relative strength relationship between fatigue expansion and self-healing recovery.

It is worth noting that the nano content is not necessarily the higher the better. The results show that under a 1.0% nano content condition, the material performs best in terms of fatigue life, healing recovery rate, and competition state coefficient. Although the 1.5% nano content group still outperforms the unmodified group, some indicators have declined. This indicates that nano materials can play an interface-enhancing and structural-coordinating role within an appropriate range, but when the content is too high, local agglomeration, uneven dispersion, and discontinuous phase-state problems will gradually emerge, thereby weakening their positive regulatory effect on the fatigue-healing competition relationship. Thus, in material design, more attention should be paid to the threshold of content and structural balance, rather than solely focusing on improving individual performance.

Furthermore, the influence of recovery temperature and recovery time on the competition state is also significant. Moderate heating helps to increase molecular migration activity and interface reorganization efficiency, enabling the system to gradually shift from fatigue dominance to competitive equilibrium or even healing dominance. However, when the temperature is too high, the competition state coefficient of some groups declines, indicating that structural softening and local instability will re-weaken the recovery advantage [19]. This phenomenon suggests that the fatigue-healing competition relationship has a clear conditional dependence, and the performance of the material is not only determined by the ratio itself, but also by the environment and recovery conditions during the service process [20].

Overall, the cross-scale analysis method established in this paper can better reveal the formation path of the fatigue-healing competition mechanism of nano-modified natural asphalt. However, at present, the consideration of complex service environments, long-term aging, and multiple cycle recovery conditions is still relatively limited. Further verification is still needed by combining longer cycles and more complex working conditions in the future.

## 6 Conclusion

This paper focuses on the fatigue-healing competition behavior of nano-modified natural

asphalt and establishes a cross-scale characterization, competition state discrimination, and experimental-simulation collaborative calibration method. The research shows that the synergistic modification of natural asphalt and nano materials can enhance interface continuity and structural stability, and improve service performance through molecular diffusion, interface reorganization, and damage inhibition. The G3 group has the best comprehensive performance, with a dynamic modulus of 2.36 GPa, a fatigue life of  $7.10 \times 10^4$  cycles, a healing recovery rate of 66.9%, and a competition state coefficient of 0.21; the contribution of recovery temperature is the highest, at 29.4%. The model prediction is in good agreement with the experimental results, indicating that the established method can accurately represent the dynamic balance relationship between fatigue expansion and self-healing recovery, and can provide support for the ratio design, parameter optimization, and intelligent road performance prediction of nano-modified natural asphalt materials.

## Funding

This work was supported by University Technology Malaysia, UTM

## References

- [1] Chaudhary M, Ali A, Mehta Y, et al. Influence of Nano-Modifiers on Healing and Fatigue Properties of Asphalt Binders: [J]. *Transportation Research Record*, 2025, 2679(11): 526-539. DOI:10.1177/03611981251348447.
- [2] Chen X, Zhang J, Liu Z, et al. Self-healing analyses of steel slag asphalt mixture under microwave heating through multi-scale laboratory tests [J]. *Construction and Building Materials*, 2025, 460. DOI:10.1016/j.conbuildmat.2024.139851.
- [3] He Z, Xie T, Chen C, et al. Physical and anti-aging characteristics of nano-TiO<sub>2</sub>/irganox 1010 composite modified asphalt [J]. *Materials express: an international journal on multidisciplinary materials research*, 2021(10):11. DOI:10.1166/mex.2021.2076.
- [4] Yuan Y, Lin M, Xu S, et al. Analysis of the self-healing mechanism of TB compound-modified asphalt based on molecular dynamics [J]. *Case Studies in Construction Materials*, 2024, 21:e03580. DOI:10.1016/j.cscm.2024.e03580.
- [5] Shu Z, Dai Z, Li L, et al. Fatigue-induced degradation of self-healing properties of asphalt mixtures: Mechanisms and quantitative characterization [J]. *Construction and Building Materials*, 2025, 492(000). DOI:10.1016/j.conbuildmat.2025.142865.
- [6] Qinbao L, Yan Z, Honggang G, et al. Graphene Oxide on Rheological and Self-healing Properties of Modified Asphalt [J]. *Journal of Materials Science & Engineering (1673-2812)*, 2025, 43(1). DOI:10.14136/j.cnki.issn1673-2812.2025.01.012.
- [7] Zhang Q, Cui Y, Qiu H. Microstructure, Fatigue, and Self-Healing Properties of SBS-Modified Asphalt under Ultraviolet Radiation [J]. *Journal of Materials in Civil Engineering*, 2023, 35(7):10. DOI:10.1061/JMCEE7.MTENG-15454.
- [8] Yang H, Ouyang J, Feng L, et al. Fatigue-Healing Performance Evaluation of Fiber-Modified Asphalt Mixture [J]. *Journal of Materials in Civil Engineering*, 2024,

- 36(1):9.DOI:10.1061/JMCEE7.MTENG-16828.
- [9] Zhang T, Gao S, He Y, et al. Effect of aging on structure and properties of self-healing-enhanced SBS modified asphalt with dual dynamic chemical bonds[J]. *Materials Today Communications*, 2025, 42(000).DOI:10.1016/j.mtcomm.2024.111303.
- [10] Tehrani F F, Petit C, Sawda C E, et al. Heterogeneous numerical simulation of fatigue behaviour of porous HMA by a multi-scale approach[J]. *Road Materials and Pavement Design*, 2023, 24(sup1):690-705.DOI:10.1080/14680629.2023.2186134.
- [11] Al-Hamdou A M, Albayati A H. Fatigue performance of asphalt binders modified with varying nanomaterials[J]. *Results in Engineering*, 2025, 28(000).DOI:10.1016/j.rineng.2025.107238.
- [12] Men B, Li X, Sha T, et al. Research on Fatigue Performance of Fast-Melting SBS/Epoxy Resin Composite-Modified Asphalt[J]. *Coatings (2079-6412)*, 2024, 14(7).DOI:10.3390/coatings14070789.
- [13] Adnan A M, Wang J. Investigation of the effects of nano-Al<sub>2</sub>O<sub>3</sub> addition on compatibility, rutting and fatigue properties of styrene-butadiene-rubber modified asphalt[J]. *Construction and Building Materials*, 2024, 416(000):20.DOI:10.1016/j.conbuildmat.2024.135267.
- [14] Qu L, Wang Y, Riara M, et al. Study on fatigue-healing performance and life prediction of hot recycled asphalt mixture[J]. *Construction and Building Materials*, 2024, 436(000):14.DOI:10.1016/j.conbuildmat.2024.136964.
- [15] Yue M, Yue J, Wang R, et al. Evaluating the fatigue characteristics and healing potential of asphalt binder modified with Sasobit and polymers using linear amplitude sweep test[J]. *Construction and Building Materials*, 2021, 289(2):123054.DOI:10.1016/j.conbuildmat.2021.123054.
- [16] Li L, Wu C, Cheng Y, et al. Laboratory investigation on viscoelastic and fatigue properties of diatomite modified asphalt based on dynamic shear rheometer[J]. *Construction and Building Materials*, 2022, 327:126940-.DOI:10.1016/j.conbuildmat.2022.126940.
- [17] Shi C, Cai X, Wang T, et al. Energy-based characterization of the fatigue crack density evolution of asphalt binders through controlled-stress fatigue testing[J]. *Construction and Building Materials*, 2021(Sep.20):300.DOI:10.1016/j.conbuildmat.2021.124275.
- [18] Radziszewski P, Pokorski P, Liphardt A, et al. The influence of fiber addition on fatigue life of mineral-asphalt composites for road pavement layers constructed using hot and warm mix asphalt technology[J]. *Roads & Bridges / Drogi i Mosty*, 2025, 24(4).DOI:10.7409/rabdim.025.024.
- [19] Zheng C, Cheng P, Li Y, et al. Measurement and characterization of asphalt fatigue behavior under multi-factor effects[J]. *Materials and Structures*, 2024, 57(9):16. DOI:10.1617/s11527-024-02473-0.
- [20] Sun Y, He D, Li J. Research on the Fatigue Life Prediction for a New Modified Asphalt Mixture of a Support Vector Machine Based on Particle Swarm Optimization[J]. *Applied*

Sciences (2076-3417), 2021, 11(24).DOI:10.3390/app112411867.